AEM
Journals.ASM.org

Field and Experimental Evidence of *Vibrio parahaemolyticus* as the Causative Agent of Acute Hepatopancreatic Necrosis Disease of Cultured Shrimp (*Litopenaeus vannamei*) in Northwestern Mexico

Sonia A. Soto-Rodriguez, Bruno Gomez-Gil, Rodolfo Lozano-Olvera, Miguel Betancourt-Lozano, Maria Soledad Morales-Covarrubias

CIAD, AC Mazatlan Unit for Aquaculture and Environmental Management, Mazatlan, Sinaloa, México

Moribund shrimp affected by acute hepatopancreatic necrosis disease (AHPND) from farms in northwestern Mexico were sampled for bacteriological and histological analysis. Bacterial isolates were molecularly identified as *Vibrio parahaemolyticus* by the presence of the *tlh* gene. The *tdh*-negative, *trh*-negative, and *tlh*-positive *V. parahaemolyticus* strains were further characterized by repetitive extragenic palindromic element-PCR (rep-PCR), and primers AP1, AP2, AP3, and AP and an ems2 IQ2000 detection kit (GeneReach, Taiwan) were used in the diagnostic tests for AHPND. The *V. parahaemolyticus* strains were used in immersion challenges with shrimp, and farmed and challenged shrimp presented the same clinical and pathological symptoms: lethargy, empty gut, pale and aqueous hepatopancreas, and expanded chromatophores. Using histological analysis and bacterial density count, three stages of AHNPD (initial, acute, and terminal) were identified in the affected shrimp. The pathognomonic lesions indicating severe desquamation of tubular epithelial cells of the hepatopancreas were observed in both challenged and pond-infected shrimp. The results showed that different *V. parahaemolyticus* strains have different virulences; some of the less virulent strains do not induce 100% mortality, and mortality rates also rise more slowly than they do for the more virulent strains. The virulence of *V. parahaemolyticus* strains was dose dependent, where the threshold infective density was 10^4 CFU ml^{-1}; below that density, no mortality was observed. The AP3 primer set had the best sensitivity and specificity. Field and experimental results showed that the *V. parahaemolyticus* strain that causes AHPND acts as a primary pathogen for shrimp in Mexico compared with the *V. parahaemolyticus* strains reported to date.

Shrimp farming in Mexico has developed rapidly in recent years. In 2005, Mexico produced a total of 90,041 tons (39) (http://www.conapesca.sagarpa.gob.mx/wb/cona/cona_produccion_pesquera_y_acuicola_2005), and the volume of production in 2011 showed an increase of 18% to 109,815 tons. Mexican shrimp production depends mainly on the northwestern states, and Sonora, Sinaloa, Nayarit, and Baja California reported a joint production in 2011 of 105,218 tons, which was worth 4.263 billion Mexican pesos (40) (http://www.conapesca.sagarpa.gob.mx/wb/cona/anuario_2011). Unfortunately, the rapid growth of this industry has increased the number of epizootics associated with infectious diseases in Mexico and other countries in Latin America, and significant losses of shrimp production have occurred because of disease caused by viruses, such as infectious hypodermal and hematopoietic necrosis virus (IHHNV), Taura syndrome virus (TSV), and white spot syndrome virus (WSSV) (1), and bacteria, such as the necrotizing hepatopancreatitis bacterium (NHP-B) (2, 3) and *Vibrio* (4). Vibriosis is a disease caused by bacteria belonging to the *Vibrio* genus that produce necrotic lesions in the tissues of infected organisms (5, 6). This disease is important for the Sinaloa shrimp farms because of recurrent infectious outbreaks in recent years (4). In most cases, however, *Vibrio* bacteria are considered opportunistic pathogens for shrimp. In addition, there are emerging infectious diseases that have appeared recently or experienced rapid increases in geographic range, and the risk of disease may increase in the future. In 2013, shrimp farms from northwest Mexico were affected by atypical mortalities that occurred primarily in the first days after stocking. In the first culture cycle of the Nayarit State shrimp farms, atypical mortalities were registered in the first 30 days of culture. Mortalities with the same characteristics were subsequently observed in Sinaloa and Sonora states, and they affected regional production and produced economic losses of over 2.5 million pesos (Julio Cabanillas, personal communication, 29 May 2013). The industry in Mexico was deeply affected because of the large scale of the mortalities and lack of response to antibiotics commonly used in shrimp farming (7), such as enrofloxacin, oxytetracycline, and florfenicol. Between 0.2 and 2.5 g of diseased shrimp was collected from affected ponds, and a preliminary assessment revealed clinical signs that included anorexia, lethargy, and discoloration of the hepatopancreas (HP); moreover, a histological analysis revealed damage to the hepatopancreas characterized by severe necrosis of the tubular epithelium, with certain animals showing a heightened inflammatory response and melanization of the tubular tissue. In addition, microbiological analyses indicated a low presence of bacteria in the hemolymph (HL) and HP and a high load of *Vibrio* bacteria in the stomach (ST). Field and laboratory observations have been similar to those in reports from Asia for early mortality syndrome (EMS)

Received 31 October 2014 **Accepted** 15 December 2014

Accepted manuscript posted online 29 December 2014

Citation Soto-Rodriguez SA, Gomez-Gil B, Lozano-Olvera R, Betancourt-Lozano M, Morales-Covarrubias MS. 2015. Field and experimental evidence of *Vibrio parahaemolyticus* as the causative agent of acute hepatopancreatic necrosis disease of cultured shrimp (*Litopenaeus vannamei*) in northwestern Mexico. Appl Environ Microbiol 81:1689–1699. doi:10.1128/AEM.03610-14.

Editor: M. W. Griffiths

Address correspondence to Sonia A. Soto-Rodriguez, ssoto@ciad.mx.

doi:10.1128/AEM.03610-14

(8). In 2011, a more descriptive name was proposed for the disease that affects *Litopenaeus vannamei* and *Penaeus monodon* shrimp, which is now referred to as acute hepatopancreatic necrosis syndrome (AHPNS) (18) and has been reported in Mexico as acute hepatopancreatic necrosis disease (AHPND) (10).The goal of this study was to obtain evidence that *Vibrio parahaemolyticus* is the causal agent of AHPND in shrimp farms from northwest Mexico through the use of field studies in farms and with laboratory assays that fulfill Koch's postulates.

MATERIALS AND METHODS

Sample collection and bacterial isolation. To fulfill Koch's first postulate (the microorganism or other pathogen must be present in all cases of the disease), field samples were taken to isolate the bacteria. Ten sample collections were conducted on 20 farms from Angostura, Eldorado, Ahome, El Rosario, and Escuinapa. In addition, wild shrimp were collected from two coastal lagoons of Sinaloa: Cospita (24°6′13.36″N, 107°7′27.30″W) and Huizache-Caimanero (two sites, at 22°52′51.54″N, 106°3′58.69″W, and 22°54′0.55″N, 106°0′47.22″W).

Shrimp affected by AHPND presented clinical signs based on the severity of infection, including empty gut, anorexia, lethargy, expanded chromatophores, and pale HP with discoloration. Diseased shrimp were collected and transported inside iceboxes in plastic bags filled with pond water. The samples were immediately transported to a bacteriology laboratory. Ice was placed around the bags to lower the temperature during the transportation when the time to the laboratory was more than 4 h.

Bacteriology, virology, and histopathology analyses were performed and samples prepared for wet mount for 175 shrimp from 26 April to 24 September 2013.

The shrimp were analyzed individually; each shrimp was disinfected with 70% ethanol, and the abnormalities and weight were recorded. HL was withdrawn from the ventral sinuses of >1 g shrimp using a 1.0-ml syringe and inoculated onto thiosulfate-citrate-bile-sucrose (TCBS) agar (Difco, Lawrence, KS, USA). Subsequently, the shell was removed and the intestine (IN), ST, and HP were dissected aseptically. The IN and pieces of the ST and HP (depending on the size of the tissue) were fixed in 96% ethanol for metagenomic analysis. The remainder of the ST and HP were weighed and homogenized in 10 or 1.0 ml sterile saline solution (SSS) (2.5% NaCl). Serial 10-fold dilutions of the supernatant with SSS were produced; 0.1 ml of the solution was inoculated onto TCBS agar to enumerate the *Vibrio* spp., and 0.1 ml was inoculated onto marine agar for the heterotrophic bacteria. All of the plates were incubated at 30°C for 24 h, and then the CFU were counted and yellow colonies (YCs) and green colonies (GCs) were recorded. The results are reported as CFU ml^{-1} and CFU g^{-1} for HL and HP, respectively, and as percent GC HL and GC HP. Four to six shrimp were analyzed from each sampled pond, and the remaining HP was fixed for histology.

Histological analysis. The hepatopancreas lesions related to the disease were identified by histopathological analysis. Hepatopancreatic tissue was excised from 6 to 12 shrimp per pond and preserved in Davidson's fixative for 48 h before processing by routine histology (11). The tissue sections were stained with hematoxylin and eosin (H&E).

Isolation of bacteria. To fulfill Koch's second postulate (the pathogen can be isolated from the diseased host and grown in pure culture), bacteria were isolated from shrimp samples. The GCs from the TCBS agar plates were further purified in TCBS, CHROMagar Vibrio (CHROMagar, Paris, France), and tryptic soy agar (TSA) (Bioxon) supplemented with 2.0% NaCl. The plates were incubated at 30°C for 18 to 24 h, and selected pure isolates were then cryopreserved at −80°C in tryptic soy broth (TSB) (Bioxon) with 15% (vol/vol) glycerol.

DNA was extracted from the bacterial isolates with the Wizard DNA purification kit (Promega, Madison, WI, USA) according to the manufacturer's instructions, and the DNA was spectrophotometrically adjusted to 50 ng μl^{-1}.

Molecular identification and characterization of the isolates. All of the suspected colonies were analyzed for the presence of the molecular markers of *V. parahaemolyticus*, i.e., the thermolabile hemolysin (*tlh*), thermostable direct hemolysin (*tdh*), and thermostable direct hemolysin-related (*trh*) genes, as described by Bej et al. (12). Only isolates positive for *tlh* but negative for *tdh* and *trh* were further analyzed by PCR following the previously described methodology (13, 14) with AP1, AP2, and AP3 primers; these primers target contigs that belong to a plasmid in pathogenic strains isolated in Thailand. Another set of primers that target contig JALL01000078 of a potentially conjugative plasmid (AP) of strain M06-05 (15) was also tested. Primers 39132f (CTTCGCGGCAGCTTGAACGG) and 39627r (CGCTGCTTGTGTTTGGCGGTT) were used in PCRs run at 95°C for 5 min followed by 35 cycles of 95°C for 35 s, 60°C for 35 s, and 72°C for 90 s and a final extension at 72°C for 10 min with an Axygen PCR plate (Corning, Tewksbury, MA, USA). A commercial ems2 IQ2000 kit (GeneReach, Taiwan) was also used according to the manufacturer's instructions to test the strains.

The sensitivity, specificity, and predictive values for each diagnostic test were estimated using bacterial pathogenicity (strains that cause mortality associated with the typical histological lesions of the disease) as the standard. For this analysis, only strains confirmed as pathogenic (nine strains) or nonpathogenic (eleven strains) were used. The true-positive, true-negative, false-positive, and false-negative values were analyzed using the software Working in Epidemiology (http://www.winepi.net/uk/index.htm).

For the genomic characterization of the *tlh*-positive, *tdh*-negative, and *trh*-negative isolates, DNA fingerprinting was performed with repetitive extragenic palindromic element-PCR (rep-PCR) using the GTG_5 primer or enterobacterial repetitive intergenic consensus (ERIC) (16) with *Taq* polymerase (5 U; Promega) in a MyCycler thermal cycler (Bio-Rad, Hercules, CA, USA). The PCR products were electrophoresed in 2.25% 20- by 20-cm agarose gels (Promega) in 0.5× Tris-acetate-EDTA (TAE) buffer for 260 min at 70 V and 4 to 8°C. The gels were stained with GelRed (Biotium, Hayward, CA, USA) and visualized in a gel documentation system (UVP, Upland, CA, USA). The resulting TIFF files were analyzed using the GelCompar II software (version 4.5; Applied Maths, Austin, TX, USA). The similarity matrix was calculated with the Jaccard coefficient as recommended by Kosman and Leonard (17), and the dendrogram was constructed using the Ward algorithm. The isolates were considered to be from the same strain if they had over 95% similarity.

Experimental infections. (i) Bacterial inocula. The bacterial inocula were obtained from EMS-positive (EMS^+) and EMS-negative (EMS^-) isolates (ems2 IQ2000; GeneReach, Taiwan). The bacteria were recovered from the cryovials, inoculated in 10 ml of TSB (Bioxon, Mexico) supplemented with 2.0% NaCl, and incubated overnight at 30°C. One hundred microliters was inoculated into flasks containing 30 ml of sterile TSB plus 2.0% NaCl, and the flasks were then placed in a rotary shaker and incubated for 18 h at 30 to 31°C. After 18 h of incubation, the TSB suspensions were checked using a spectrophotometer at an optical density (OD) of 600 nm to determine the bacterial density, which was between 10^7 and 10^8 cells ml^{-1}. These suspensions were plated onto TCBS (Bioxon, Mexico) after serial dilution to determine the CFU ml^{-1} of the isolates.

(ii) Bath challenges with the isolates. Koch's third postulate (the pathogen from the pure culture must cause the disease when inoculated into a healthy, susceptible laboratory animal) was fulfilled by immersion challenge with healthy shrimp. The challenges were conducted as described by Tran et al. (18) with certain modifications, and selected EMS^+ and EMS^- isolates were used. Briefly, 5 to 7 shrimp weighing from 1.0 to 4.0 g were immersed for 15 min and aerated in a flask containing 300 ml or 500 ml of sterile seawater (control group), sterile TSB plus 2.0% NaCl (negative-control group), or the previously prepared bacterial suspension. Following immersion, the bacterial suspension including shrimp was added directly into an experimental tank that was filled with filtered seawater (10 μm) at a salinity of 35 ppt and aerated. The experiment was conducting under a 12-h light/dark photoperiod. The water temperature

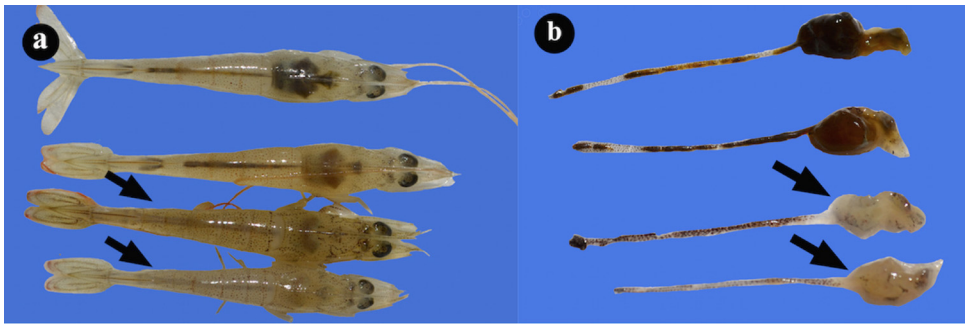

FIG 1 (a) Photographs of hepatopancreases from healthy *L. vannamei* shrimp and shrimp naturally infected with AHPND (arrows). (b) The hepatopancreas without external membrane shows atrophy and white color.

was maintained at approximately 29 ± 1°C, the dissolved oxygen was maintained above 5 ppm, and the pH was 8.1 ± 0.2. The final bacterial density in the tank was approximately 10^6 cells ml^{-1} with three replicates. Eleven EMS^+ and three EMS^- isolates were tested with this procedure.

(iii) Observation and sampling. The shrimp were fed a pelleted shrimp feed (35% protein; Purina) twice daily during the bioassay period and the were checked every hour until all of the shrimp died. Moribund shrimp were disinfected with 70% ethanol, and the IN, HP, and ST were dissected aseptically for the bacteriological and histological analyses as previously described.

(iv) Reisolation of bacteria and molecular identification. To assess Koch's fourth postulate (the pathogen must be reisolated from the new host and shown to be the same as the originally inoculated pathogen), the HP, IN, and ST samples from moribund organisms with pale HP were collected within 24 h postinfection (p.i.). The samples were inoculated on TCBS agar and incubated at 30°C for 24 h. GCs were plated on CHROMagar Vibrio, and the DNA of the mauve-colored colonies was fingerprinted by rep-PCR (19) for subsequent comparisons with the tested isolates.

(v) Infectious dose. To find the bacterial density below which no mortality was observed, an infection density assay was done. A modification to the challenges described by Tran et al. (18) was performed using the pathogenic strain M09-04. Bacterial inocula were added directly into an experimental tank containing 10 shrimp weighing 1.15 ± 0.04 g. The tanks were filled with filtered seawater (10 μm) at a salinity of 35 ppt and then aerated. Six bacterial densities were tested: 7.80×10^1, 7.85×10^2, 7.85×10^3, 8.20×10^4, 8.26×10^5, and 8.10×10^6 CFU/ml. For the control group, sterile TSB plus 2.0% NaCl was used. Three replicates were performed for the treatments and control groups, and the experiment was conducted under a 12-h light/dark photoperiod. The water temperature was maintained at 29 ± 1°C, the dissolved oxygen was maintained above 5 ppm, and the pH was 8.1 ± 0.2.

RESULTS

Gross signs in farmed shrimp infected with AHPND. The average body weight of the affected shrimp ranged from 0.1 to 8.0 g on the day of sampling. Moribund shrimp collected from farms affected with AHPND presented slightly expanded chromatophores, lethargy, erratic swimming, and empty guts. Diseased shrimp typically presented HP discoloration and an organ with an aqueous consistency (Fig. 1), and as the infection developed, the organ consistency became rubbery. After the dark membrane that overlays the HP was removed, a pale-colored organ was observed.

Histopathology of the disease from shrimp farms. Symptomatic shrimp showed a severe necrosis of the HP tubules with a massive sloughing of epithelial cells that caused disorganization and a total loss of tissue structure (Fig. 2). The histological analysis determined three stages of AHPND: initial, acute, and terminal. In the initial stage, the epithelial cells are elongated into tubular lumen and look like "drops" (Fig. 2b and c). In addition, there is a reduction of the vacuole size from R and B cells as the infection progresses (Fig. 2d), and there is also an increased desquamation of tubular epithelial cells through the acute stage (Fig. 2e to h).

In the acute stage of the disease, the tubular epithelium is necrotic with a severe desquamation of the cells, which accumulate in the lumen as dead cells (Fig. 2e and f). As the infection develops, an increase in the number of damage tubules is observed until the entire organ is affected (Fig. 2g). Severely affected tubules show hemocytic infiltration as a response to the necrotic epithelium (Fig. 2h).

In the terminal stage of the disease, the intertubular tissue from the HP tubules shows a severe inflammatory response, and the tubular epithelium becomes entirely necrotic, with dead cells at different phases of lysis (Fig. 3a), which causes a proliferation of bacterial masses inside the tubule lumens (Fig. 3b). The interstitial spaces from these tubules show an increased hemocytic infiltration that develops hemocytic capsules around the tissues. As the infection proceeds, certain tubules present melanization from the necrotic material, and the tissues develop more severe lesions and increased bacteria inside the tubular lumen (Fig. 3c), which results in an inflammatory response and melanization (Fig. 3d).

Densities of *Vibrio* spp. and total heterotrophic bacteria in farmed shrimp. The highest mean bacterial densities were determined in the STs of the shrimp (Table 1) for both heterotrophic bacteria and *Vibrio* spp. No significant differences were observed between the bacterial densities on TCBS and marine agars among the shrimp at the disease stages for the ST (TCBS agar, $P = 0.109$; marine agar, $P = 0.113$) or HP (TCBS agar, $P = 0.131$; Marine agar, $P = 0.074$).

An increase in *Vibrio* sp. density was observed as the infection progressed from normal shrimp appearance to the terminal stage, and there was a dominance of YCs; however, the GCs on TCBS were from 20 to 38% for the HP and from 13 to 42% for the ST (Table 2). As Tran et al. (18) reported, *V. parahaemolyticus* is the causal agent of AHPNS/EMS in Asia, and our strategy was to collect samples for diagnosis; therefore, only shrimp in the early days of stocking with clear signs of the disease and in the initial stages of infection were sampled. From these samples, GCs on TCBS and mauve colonies on CHROMagar were selected to obtain the bacterial isolates that were later characterized by molecular methods.

Characterization and identification of isolates from shrimp farms affected by AHPND. In total, 294 bacterial isolates were

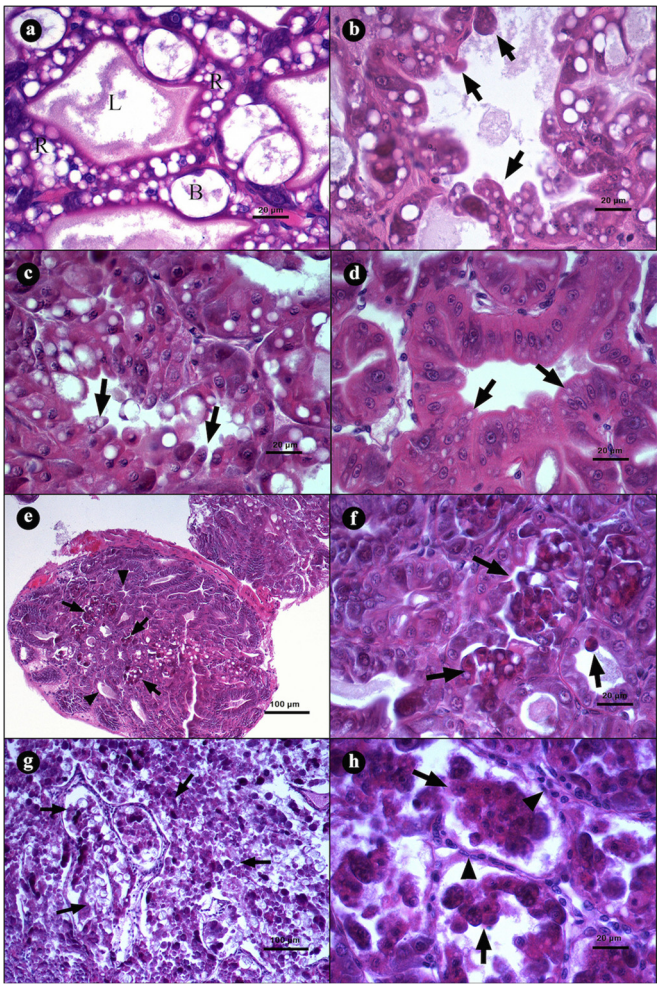

FIG 2 Microphotographs of hepatopancreases (HPs) from *L. vannamei* naturally infected by AHPND. (a) Transversal view of HP with a clear lumen (L), R and B cells, and a normal tubular epithelium. (b to d) Initial stage of infection. (b and c) Transversal view of tubules with elongation of epithelial cells (arrows) toward the lumen. (d) Tubular epithelium with strong reduction of vacuoles in R and B cells (arrows). (e to h) Acute stage of infection. (e) Tubules with a reduction of vacuoles in R and B cells (arrowheads) and severe desquamation of the epithelium (arrows). (f) Magnification of panel e, showing a tubular epithelium necrosis with dead cells inside the lumen (arrows). (g) Severe organ disorganization caused by desquamation of the tubular epithelium. (h) Incipient hemocytic infiltration (arrowhead) in the interstitial spaces of the tubules and loss of continuity of the epithelium due to the necrotic process (arrows). Hematoxylin and eosin staining was used. Microphotographs by S. Abad.

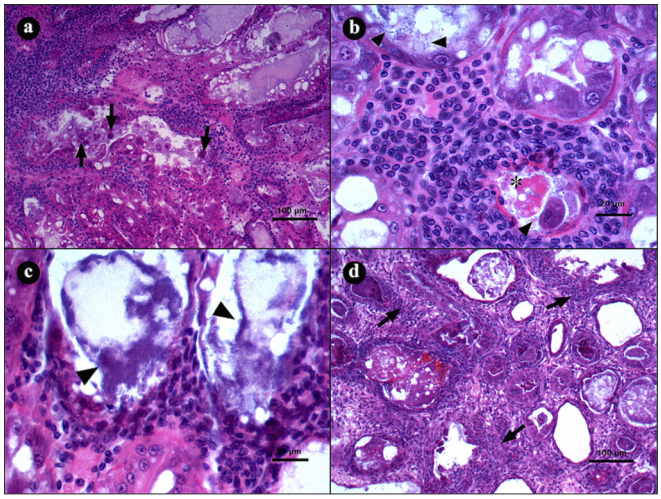

FIG 3 Microphotographs of hepatopancreases (HPs) from *L. vannamei* naturally infected by AHPND in the terminal stage of infection. (a) Transversal view of HP with severe hemocytic infiltration in the interstitial spaces as a response to epithelium necrosis (arrows). (b and c) Hepatopancreas tubule shows hemocytic infiltration, with necrotic cells (asterisk) and bacterial masses inside the lumen (arrowheads). (d) Transverse view of HP with severe hemocytic infiltration (arrow) and melanization of necrotic material inside the tubules. Hematoxylin and eosin staining was used. Microphotographs by S. Abad.

recovered from the diseased shrimp and pond water. Of these, 37 were positive for *tlh* and negative for the human-toxigenic genes *tdh* and *trh*; therefore, *V. parahaemolyticus* was presumably nontoxigenic to humans (Table 3). *V. parahaemolyticus* isolates were obtained from the HL (1 isolate), HP (14 isolates), ST (20 isolates), and pond water (1 isolate) from May (21 isolates), June (2 isolates), July (5 isolates), August (8 isolates), and one undetermined date.

The 37 *tlh*-positive, *tdh*-negative, and *trh*-negative isolates were fingerprinted using ERIC-PCR, and several clones were detected (Fig. 4a, b, and c). Clonal group a includes four isolates that were obtained from the pond water and the STs and HPs from two different shrimp collected in the same pond. Clonal group b was obtained from the STs of two shrimp from the same pond, and clonal group c was obtained from the HPs of two shrimp from different farms. All other isolates produced different results and were considered strains; in total, 31 strains were obtained.

The AP primer set produced a 495-bp amplicon in an intergenic region that was present in all pathogenic strains tested (Table 3) and in three nonpathogenic strains. The AP1 and AP2 also targeted what appeared to be the same plasmidic contig.

The highest sensitivity and specificity were for the AP3 primers used to detect AHPND (Table 3), which presented positive and negative predictive values of 90 and 100%, respectively, meaning that an organism with a positive result obtained with this test had a 90.0% probability of being a diseased organism, whereas an organism with a negative result had a 100.0% probability of being a healthy organism. The worst diagnostic test was for AP1, at positive and negative predictive values of 20 and 46.7%, respectively. The ems2 IQ2000 diagnostic kit showed positive and negative predictive values of 61.5 and 85.7%, respectively.

Bacterial challenges. The shrimp were challenged with 14 *tlh*-positive, *tdh*-negative, and *trh*-negative bacterial strains through direct inoculation of the strain in the aquaria.

The gross signs in shrimp challenged with pure strains included the same characteristics of infected *L. vannamei* from shrimp farms. Challenged shrimp showed expanded chromatophores, anorexia, and erratic swimming within the first hour postinfection. Subsequently, the shrimp showed pale and aqueous HP, empty gut, and lethargy. Discoloration and atrophy of the HP increased throughout the infection process.

Certain strains, such as M09-04 at 2.20×10^{6} CFU ml^{-1}, caused shrimp mortality after 4 h p.i. (Fig. 5), whereas other strains, such as M06-07 at 7.28×10^{6} CFU ml^{-1}, caused mortality after 10 h p.i.

TABLE 1 Bacterial density in hemolymph, hepatopancreases, and stomachs of shrimp collected from seven affected farms with AHPND in northwest Mexico

Parameter	Bacterial density in:					
	Hemolymph (CFU ml^{-1})		Hepatopancreas (CFU g^{-1})		Stomach (CFU g^{-1})	
	Marine agar	TCBS agar	Marine agar	TCBS agar	Marine agar	TCBS agar
Mean	3.65×10^2	1.19×10^1	6.62×10^7	2.59×10^7	1.00×10^8	3.27×10^7
Maximum	1.60×10^3	2.05×10^2	1.86×10^9	1.42×10^9	5.47×10^8	5.43×10^8
Minimum	0	0	1.60×10^2	0	2.25×10^2	0
SD	5.84×10^2	4.90×10^1	2.68×10^8	1.76×10^8	1.65×10^8	1.08×10^8
n	14	27	89	107	33	55

Koch's postulates were corroborated by bacterial DNA fingerprinting patterns (Fig. 6). When M09-04 was inoculated, the same DNA pattern was observed in three organs within the shrimp 1 sample (ST, 1; HP, 1; and IN, 1) and two organs in the shrimp 2 sample (ST, 2; and IN, 2). M06-03 showed the same DNA pattern as HP in the shrimp 2 sample and IN in the shrimp 3 sample. A 100% similarity was obtained with the isolates from the STs of shrimp samples 1 and 2. These values clearly demonstrate that the two inoculated strains (M09-04 and M06-03) were recovered from moribund shrimp.

Histopathology of AHPND from challenge tests. Shrimp challenged with the pure *V. parahaemolyticus* strains presented histopathological lesions that are associated with AHPND-infected shrimp in farms, whereas shrimp from the control group and challenged with nonpathogenic strains did not show any noticeable alteration in their HPs.

The acute stage of the disease was observed from 3 to 18 h p.i., which presented as a typical disorganization of the HP tubules caused by a desquamation of epithelium (Fig. 7a). Moribund organisms presented with severe necrosis of the tubular epithelium (Fig. 7b), a reduction of R and B cell vacuoles, and accumulation of necrotic cells in the lumen (Fig. 7c). As a response to the lesions, the intertubular space of certain tubules presented hemocytic infiltration, which increased as the infection progressed (Fig. 7d).

Between 18 and 24 h p.i., the shrimp showed typical lesions associated with the terminal stage of the disease (Fig. 7e to h). The HP presented severe hemocytic infiltration around affected tubules that caused melanization (Fig. 7e). The tubular epithelium was necrotic, and the lumen had a massive proliferation of bacteria (Fig. 7f), which was observed over time.

The surviving organisms after 27 h p.i. showed clear signs of melanization and hemocytic capsules (Fig. 7g). Certain tubules were fully necrotic and absent the tubular epithelium, whereas other tubules were melanized with bacterial masses in their lumens (Fig. 7h).

Infectious density. In challenges with the M09-04 strain, the median lethal times (TL_{50}) for densities of 10^6, 10^5, and 10^4 CFU ml^{-1} were 3, 21, and 46 h p.i., respectively (Fig. 8). A density of 10^4 CFU ml^{-1} caused only 63% mortality at 104 h p.i.; below that density (10^1, 10^2, and 10^3 CFU ml^{-1}) and in the control group, no mortality was observed during the test period (167 h). Moribund shrimp presented characteristic clinical signs and histopathological lesions observed in shrimp affected by AHPND.

DISCUSSION

In general, visible signs in dying shrimp (expanded chromatophores, lethargy, and empty ST and midgut) were consistent with what has been described for AHPND occurring in Asia (www.enaca.org) and, recently, in Mexico (10). However, the HP presented characteristics that are inconsistent with previous reports and showed an aqueous consistency during the first stages of the disease and a rubbery consistency in later stages of the infection (http://www.oie.int/en/) (18), which is presumably associated with organ atrophy. The massive mortality observed in farms indicates that changes in color and consistency and organ atrophy are possibly determined by the infection stage.

Similar clinical signs have been reported in cases of infection by the necrotizing hepatopancreatitis bacterium (NHP-B) (3, 20) and septic vibriosis (21), where the atrophy of the HP together with the immunological response of the shrimp is associated with necrotic lesions and tubular melanization in the HP tissue. Although certain signs are the same as those associated with diseases and syndromes caused by bacteria of the genus *Vibrio* and NHP-B found in cultured shrimp around

TABLE 2 Bacterial density in shrimp at different stages of AHPND collected from seven different affected shrimp farms

Phase	Hepathopancreas					Stomach				
		CFU[a] g^{-1}		Green colonies (%)			CFU[a] g^{-1}		Green colonies (%)	
	n	Mean	SD	Mean	SD	*n*	Mean CFU g^{-1}	SD	Mean	SD
Normal	6	5.93×10^5	8.94×10^5	38.02	48.91	6	2.23×10^6	4.85×10^6	36.35	46.62
Initial	26	1.78×10^6	3.59×10^6	25.89	43.38	27	2.95×10^7	1.01×10^8	30.70	46.56
Acute	9	1.65×10^8	1.65×10^8	20.50	27.40	8	2.93×10^6	4.87×10^6	42.84	39.92
Terminal	4	2.88×10^8	5.75×10^8	25.00	35.36	4	1.54×10^8	2.61×10^8	13.50	19.09
ND[b]	10	1.95×10^6	4.20×10^6	32.53	44.88	10	3.49×10^7	9.74×10^7	33.42	37.43

[a] In TCBS medium.
[b] ND, no determinate phase of disease.

TABLE 3 *Vibrio parahaemolyticus* strains isolated from shrimp farms affected with AHPND in northwestern Mexico[a]

Strain ($n = 20$) or parameter	Isolation date (day/mo/yr)	Source	Organ or tissue	Pathogenic	Result with:				
					ems2 IQ2000	AP1	AP2	AP3	AP
M03-E39	27/05/2013	Shrimp	ST	N	−	−	−	−	−
M03-E48	27/05/2013	Shrimp	ST	N	−	−	−	−	−
M03-E49	27/05/2013	Shrimp	ST	N	+	−	−	−	−
M03-E55	27/05/2013	Shrimp	ST	N	−	−	−	−	−
M03-E60	27/05/2013	Shrimp	ST	N	−	?	?	−	−
M03-E66	27/05/2013	Shrimp	ST	N	−	?	−	−	−
M05-28	26/06/2013	Shrimp	ST	N	+	+	−	−	+
M06-03	22/07/2013	Water	WA	Y	+	−	+	+	+
M06-04	22/07/2013	Water	WA	N	+	−	−	+	+
M06-05	22/07/2013	Shrimp	ST	Y	+	−	+	+	+
M06-06	22/07/2013	Shrimp	HP	Y	+	−	+	+	+
M06-07	22/07/2013	Shrimp	HP	Y	+	−	+	+	+
M07-02	23/08/2013	Shrimp	ST	N	−	−	−	−	−
M08-01	24/08/2013	Shrimp	ST	Y	+	−	+	+	+
M08-02	24/08/2013	Shrimp	ST	Y	+	+	+	+	+
M08-03	24/08/2013	Shrimp	HP	Y	−	−	+	+	+
M09-03	27/08/2013	Shrimp	HP	N	+	−	+	−	−
M09-04	27/08/2013	Shrimp	HP	Y	+	−	+	+	+
M09-05	27/08/2013	Shrimp	ST	Y	+	−	+	+	+
MSG-21	ND	Shrimp	HP	N	+	?	+	−	+
Sensitivity (%)					88.9	11.1	100.0	100.0	100.0
Specificity (%)					54.5	63.6	72.7	90.9	72.7
Positive predictive value (%)					61.5	20.0	75.0	90.0	75.0
Negative predictive value (%)					85.7	46.7	100.0	100.0	100.0

[a] HP, hepatopancreas; ST, stomach; N, no; Y, yes; HE, hemolymph; WA, water; ?, doubtful result; ND, no determinate phase of disease. Confidence level, 99.5%.

the world (3), a notable difference in the size of the affected shrimp is observed. For the disease described here, the majority of affected shrimp weighed less than 1 g during the first 4 weeks of shrimp culture, whereas in the case of NHP-B, the infectious outbreaks have been observed in juvenile shrimp of *L. vannamei* from 5 to 9 weeks of cultivation that weigh between 4 and 9 g (22). Another difference is the shorter time required to develop lesions. In the present study, the organisms experimentally infected by pure strains showed lesions and mortality in the initial hours postinfection; however, in NHP-B infections, the course of the disease is slower. Vincent and Lotz (23) studied NHP-B and observed that the initial symptoms of the disease appeared after 6 days p.i. and mortality occurred after 15 days p.i. (24).

Organisms affected by the pathology described in this study presented low or no levels of heterotrophic bacteria and *Vibrio* sp. densities in the HL in general, presented low densities of *Vibrio* spp. in the HP, and presented high *Vibrio* sp. densities in the ST. In systemic vibriosis, however, the *Vibrio* sp. loads were higher than 10^3 CFU ml^{-1} (4) in the HL; the HP is normally the target organ, and it showed widespread atrophy and the development of hemocytic nodules, with a portion that were melanized.

In the present study, three stages of the disease were identified in the affected shrimp from farms: initial, acute, and terminal. In the initial stage, an elongation of the HP tubular epithelium cells toward the inside of the lumen was observed, along with a drastic reduction in the number of vacuoles in the R and B cells, notably without hemocytic infiltration. Shrimp can reduce high densities of viable bacterial cells rapidly (15 min) (9). Alday-Sanz et al. (26) found a hemocytic response in *P. monodon* of less than 20 min during an infection by immersion with *V. vulnificus*. This behavior was not observed in the initial stage described here, indicating that the bacterial attack was quicker than the activation of the cellular defense system. This result is particularly relevant because innate responses in crustaceans can be triggered by minimum quantities of molecules associated with pathogens, such as bacterial lipopolysaccharides (27). Hemocytes are the first line of defense in shrimp, and upon the initial introduction of a foreign agent (pathogen or not), the cellular defense system is activated (28, 29). In the acute stage, the histopathological damages are characterized by severe desquamation of the epithelial cells of the HP tubules, which has been previously described by Tran et al. (18); in this stage, distinctive histological lesions (pathognomonic) of AHPND can be observed (which was not previously reported for syndromes associated with bacteria of the genus *Vibrio* or NPH-B). In the terminal stage of the disease, an increase in the *Vibrio* sp. counts was consistently observed, with a predominance of YCs (70%) on TCBS agar. This can be attributed to a secondary infection by opportunistic *Vibrio* spp. that proliferate in a weakened system where the HP is completely necrotic, atrophied, and possibly dysfunctional.

When the infection has become systemic, hemocytes migrate to other tissues (antennal gland, heart, lymphoid organ, and striated muscle) to fight other bacteria (25, 30). This response might explain why GCs were replaced by YCs in the TCBS as the infection progressed (unpublished data), which was observed in labo-

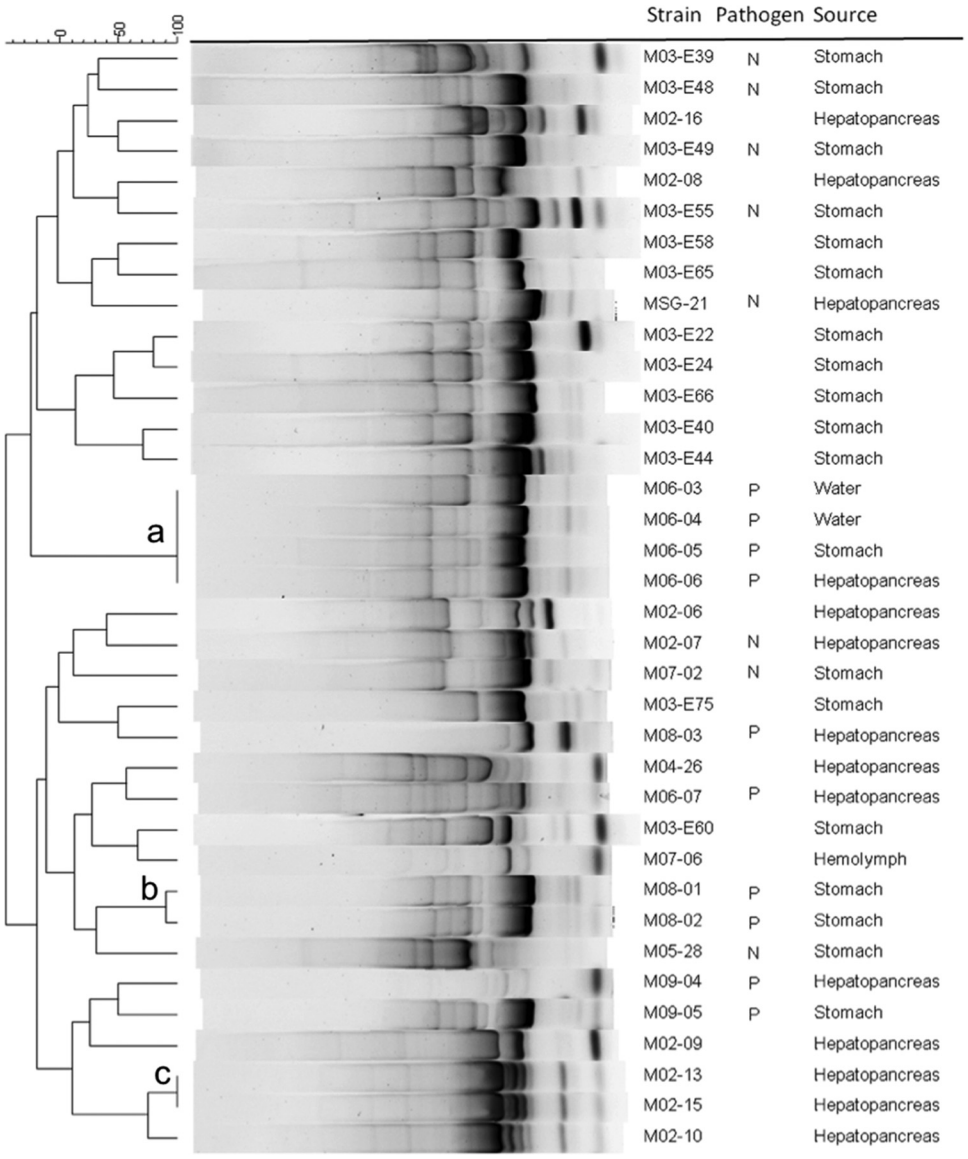

FIG 4 ERIC-PCR fingerprinting of *Vibrio parahaemolyticus* isolated from shrimp and water from ponds affected by AHPND. N, nonpathogenic; P, pathogenic. Letters in the dendrogram denote clonal groups (>95%). Band position tolerance, 1%; optimization, 0.2%.

ratory assays in which the pathogen strain M09-04 was used, and why YCs were predominant in shrimp from farms as well as in challenge assays during the terminal stage of the disease. Additional research is required to identify the predominant type of bacteria during the terminal stage and the cause of the decrease of GCs, and such research should presumably include the inoculated pathogen *V. parahaemolyticus* strain.

During the experiments with pure strains of pathogenic *V. parahaemolyticus*, the shrimp stopped feeding almost immediately postinfection (unpublished data). Subsequently, a lethargic behavior was observed, and they began to die after 4 h p.i., in certain cases with a mortality rate of 100% after 17 h p.i. (2.20×10^6 CFU ml^{-1}). The visible signs observed in dying shrimp were similar to those observed in infected shrimp from farms, and the results from the challenge assays indicated that the isolated strains had a higher virulence than the strains previously reported by Tran et al. (18), where mortality occurred at 18 h p.i. and reached 100% at 48 h p.i. Similarly, Nunan et al. (10) reported shrimp mortality that persisted for up to 4 days p.i. in immersion assays. In both studies, the methodology described by Tran et al. (18) was applied, and the approximate density in the experimental tank was 2×10^6 cells ml^{-1}.

Although the three stages of the disease were histologically observed in *per os* infection and cohabitation assays (unpublished data), the initial stage could not be observed in experiments in which pure *V. parahaemolyticus* strains were used, which indicates that *V. parahaemolyticus* could release a potent toxin capable of causing severe effects on the HP in a short period of time, such as epithelium necrosis and death during the first stages of the infection. Recently, Sirikharin et al. (14) identified two proteins (58 and 12 kDa) from extracts without cells from pathogenic strains of *V. parahaemolyticus* from Asia; these proteins were homologous

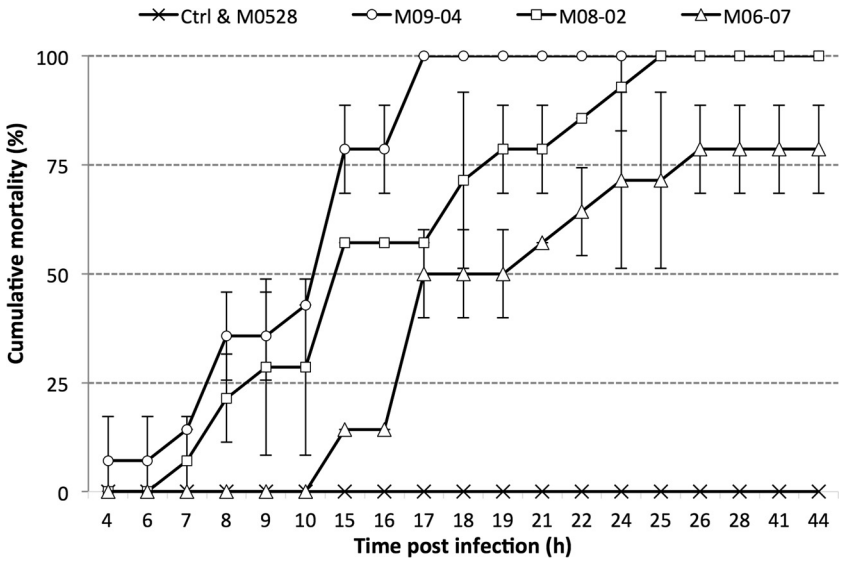

FIG 5 Example of cumulative mortality of juvenile shrimp challenged with *Vibrio parahaemolyticus* strains. M05-28, 1.20×10^7 CFU ml^{-1}; M09-04, 2.20×10^6 CFU ml^{-1}; M08-02, 3.30×10^6 CFU ml^{-1}; M06-07, 7.82×10^6 CFU ml^{-1}. Control, TSB plus 2.0% NaCl. Bars indicate standard deviations.

to bacterial toxins against insects (www.enaca.org) and are the basis upon which the first AP3 primers were developed (T. W. Flegel, personal communication). These proteins were also identified in the genome of isolated strains in the present study (15) and had significant homology to bacterial delta endotoxins PirA and PirB of *Photorhabdus luminescens*, which are highly active against insects (32).

Additionally, Tran et al. (18) distinguished three stages of the disease (acute, early terminal, and terminal) by using pure strains related to *V. parahaemolyticus* and a mixture of strains in immersion assays, and lesions similar to those reported in the present study were observed. However, these authors did not report the initial stage of the disease, which was possibly because they sampled after 48 h p.i., presumably when the initial stage had come to an end and the HP had already been severely damaged.

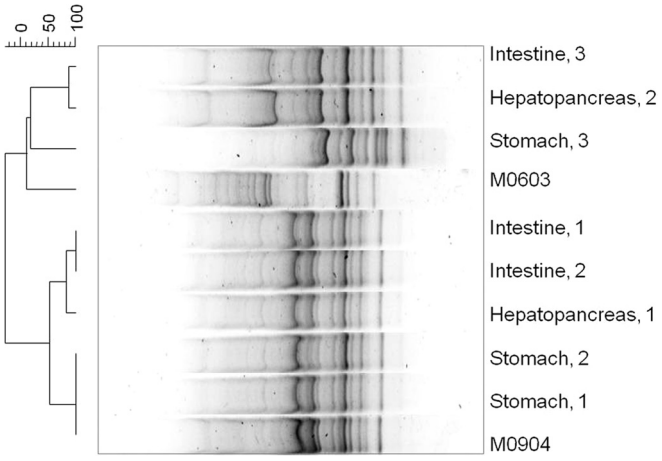

FIG 6 DNA fingerprinting of bacterial isolates obtained from challenged shrimp infected with the pathogenic *V. parahaemolyticus* strain M09-04. The organ of isolation and number of shrimp samples are shown. M09-04, strain inoculated; M06-03, strains not inoculated but used as outgroup in the GTG_5 PCR. Band position tolerance, 0.5%; optimization, 0.13%.

The acute and terminal stages that were registered experimentally showed the characteristic pathology of shrimp from farms affected by AHPND. Dying organisms in the experiment showed an acute necrosis of the HP that progressed with the disease until the organ was completely damaged and dysfunctional. In the acute stage, unlike in the initial stage, a rapid inflammatory response was observed. In the terminal stage, the HP was atrophied and completely necrotic with marked hemocytic infiltration and bacterial proliferation within the lumen of tubules. In the shrimp used in the experiments and from farms, histopathological lesions were not observed in any other organ or tissue; however, in shrimp used in experiments in which other pathogenic *Vibrio* spp. were used, the lymphoid organ, antennal gland, gills, heart, and muscle were affected (6, 21, 34). This result suggests that the epithelial cells of the HP tubules of shrimp have specific receptors for the *V. parahaemolyticus* strains that cause AHPND; therefore, research is required to determine if these receptors are located only in the HPs of the shrimp or if they are also located in the HPs of other species, which would make the species carriers of the disease.

During the challenge assays, differences in the virulence of the strains were observed. *V. parahaemolyticus* strains from clonal group a had increased virulence and exhibited the maximum levels of virulence between 7 and 10 h p.i., with mortality rates of 50% on average. In the less virulent strains (group b), the highest mortality rate was observed at 17 h p.i. A similar tendency was observed by Joshi et al. (13) in isolates of *V. parahaemolyticus* from shrimp affected by AHPND in Vietnam. The authors reported that certain strains caused 100% mortality within 24 h p.i., whereas other strains did not cause 100% mortality until 96 h p.i.; they also found that the 2HP isolate caused 75% of the mortality and produced a pathology different from that of ANHPD, such as a thinning of HP tubules and vacuolization of E cells. It is highly probable that this isolate represents a false-positive result, because it is likely that the thinning of the HP tubules is not associated with actual pathology. In addition, the AP2 system used to identify the *V. parahaemolyticus* has a low positive predictive value (75%). Therefore, two strains of *V. parahaemolyticus* AP2+ (M09-03 and

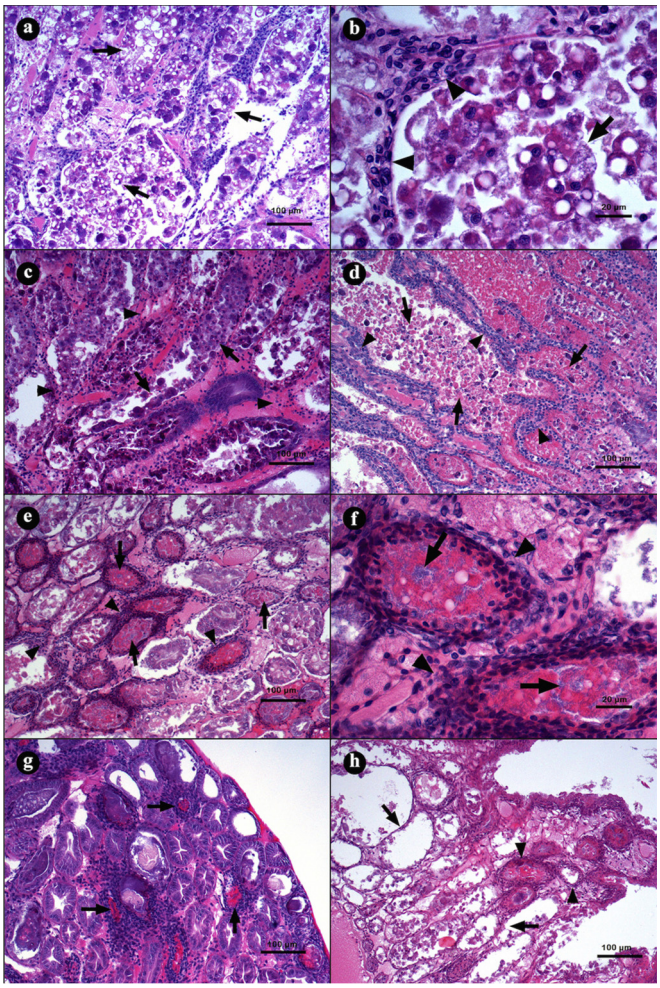

FIG 7 Microphotographs of *L. vannamei* hepatopancreases (HPs) in the acute (a to d) and terminal (e to h) stage of AHPND. (a and b) Hepatopancreas from a shrimp challenged with strain M09-05 at 3 h p.i., showing a general disorganization of the tubules due the epithelium necrosis; the lumen is full of dead cells produced by the epithelium desquamation. (b) Magnification of panel a. Epithelium desquamation and hemocytic infiltration were observed (arrowhead). (c) Hepatopancreas from a shrimp challenged with strain M08-01 at 10 h p.i., showing hemocytic infiltration (arrowhead) and reduction of R and B vacuole cells (arrow). (d) At 16 h p.i. with the same strain, the HP had a larger hemocytic infiltration (arrowhead) and accumulations of necrotic cells inside the tubular lumen (arrow). (e and f) Hepatopancreas from a shrimp challenged with strain M06-06 at 24 h p.i., with severe hemocytic infiltration (arrowhead), epithelium necrosis, deposits of melanin inside the tubular lumen, and bacterial masses (arrow). (g) Hepatopancreas from a shrimp challenged with strain M09-05 at 28 h p.i., with the largest melanization of necrotic tissue inside the tubular lumen (arrow). (h) Hepatopancreas from a shrimp challenged with strain M06-05 at 41 h p.i., showing necrotic tubules without epithelium (arrow) and tubules with hemocytic capsules (arrowhead). Hematoxylin and eosin staining was used. Microphotographs by S. Abad.

MSG21) were used in the present study, and they did not show pathogenicity in the challenge assays.

In the present study, a high diversity of pathogenic strains was observed (31 strains differentiated with rep-PCR), which suggests that the virulence of these strains or their regulators is encoded in mobile elements that might have been transferred between *V. parahaemolyticus* strains. Additional research should be performed to determine if the aforementioned transference occurs in this case and if it occurs in other strains of the Harveyi clade or other bacteria.

The diagnostic tests are important because a positive predictive value indicates the true probability of an organism being diseased, whereas a negative value indicates the true probability of an organism not being diseased. The evaluation of these tests clearly showed that the diagnostic tests based on the first AP3 had the highest degree of differentiation between the pathogenic and nonpathogenic strains of *V. parahaemolyticus*. However, AP3 showed a false-positive result in this study (strain M06-04) and produced a predictive positive value of 90%. These results differ from those reported by Sirikharin et al. (14), who showed predictive values of 100% using Asian strains. However, it is important to note that the ems2 IQ2000 diagnostic test is capable of detecting 61.5% of positive samples. Therefore, further research is required to improve the diagnostic tests and identify different regions between the genomes of nonpathogenic strains and pathogenic strains to identify false positives. If such work is achieved, proper sanitary and control measures can be implemented to prevent or halt the spread of the disease.

The results obtained in the present study demonstrate that the virulence of the *V. parahaemolyticus* strains is associated with multiple factors. In general, virulence is dependent on the strain, density, infection route, exposure time, species considered, and age and general condition of the shrimp (26, 30, 37). In this case, the virulence of the *V. parahaemolyticus* AHPND strains was clearly dependent on density, time, and type of exposure. For instance, in the immersion method when shrimp were exposed for 15 min at a high bacterial density, the M09-04 strain caused 50% mortality at 46 h p.i. with a density of 10^4 CFU ml^{-1}, whereas 93% mortality was observed with a density of 10^5 CFU ml^{-1}. This result is relevant because the water used to culture shrimp in Sinaloa normally has *Vibrio* sp. densities higher than 10^5 CFU ml^{-1} (unpublished data). It is clear that alternative strategies are required to maintain *V. parahaemolyticus* levels in tanks below density values that could be potentially pathogenic, thus minimizing the toxigenic effect of these strains. Parallel experiments (data not shown) showed that the disease is transmitted orally through the digestive tract, by cannibalism of ill shrimp, and through particulate matter located at the bottom of ponds containing affected shrimp. These results are consistent with those reported by the Food and Agriculture Organization (FAO) of the United Nations (38) and indicate that the bacteria spread through the pond water during its infectious period. Preliminary experiments also showed that mortality associated with the disease ceases when organisms are transferred to clean water, despite the organisms showing clear symptoms of the disease. However, these shrimp showed an important reduction in the size of vacuoles in the tubular epithelium and desquamated cells in the tubule lumen after the fifth day, which was presumably related to a process of reinfection.

In addition, preliminary experiments using water and detritus from affected ponds taken 41 h after an epidemic event did not cause death in healthy shrimp, which suggests that detritus from the bottom of the pond plays a major role in bacterial infection. It is likely that after 41 h, bacterial multiplication stops, and then densities fall below the infective threshold. This explanation is consistent with observations made by shrimp farmers, who reported a sudden reduction in pond mortality after an infectious outbreak.

The results of this study show clear evidence that the *V. para-*

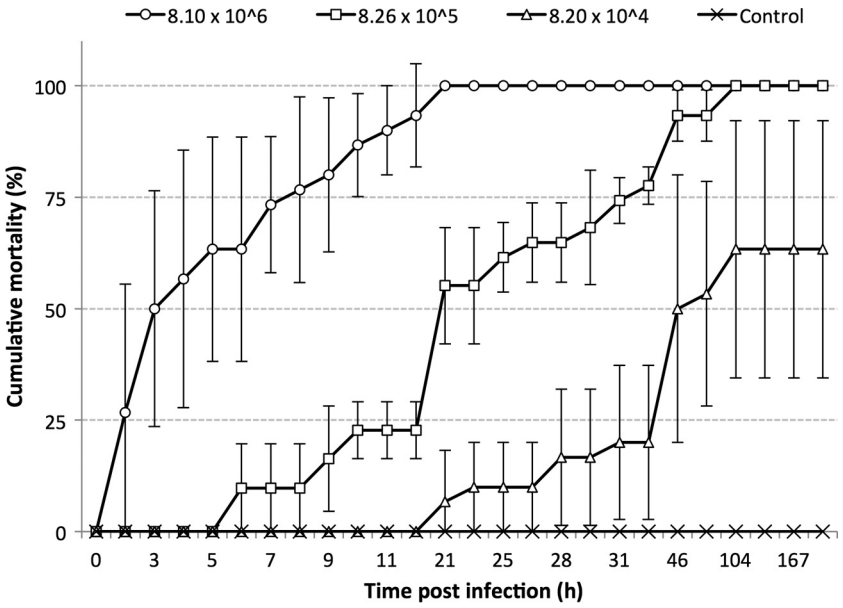

FIG 8 Cumulative mortality of juvenile shrimp challenged with *Vibrio parahaemolyticus* strain M09-04 at different bacterial densities (CFU ml^{-1}). Bars indicate standard deviations.

haemolyticus AHPND strains isolated in Mexico act as a primary pathogen in shrimp; in addition, these strains are transmitted orally during their infectious period, and they are found primarily in the HP and ST and cause the same pathognomonic lesions in both cultured shrimp and shrimp subjected to experimentation. Similar to other pathogenic bacteria, pathogenic *V. parahaemolyticus* uses the quorum-sensing system (15), likely to maintain an infective density (above 10^4 CFU ml^{-1}) at which a toxin that causes lesions and dysfunction of the HP (14) is presumably released. As the infection progresses, the HP is atrophied to such a degree that it causes the death of the organism, but the population of bacteria decreases (which could be associated with the intervention of lytic phages of bacteria). Apparently, a certain bacterial density must be reached to express pathogenicity, which might occur through the release of a toxin. Additional studies are required to test this hypothesis and determine if the toxin can remain active in water. The focus of subsequent studies can also include determining host-pathogen interactions as well as isolating and characterizing the toxin that causes the disease. Improvements in diagnostic field tests may permit monitoring farm outbreaks in detail and identifying the main environmental factors that cause outbreaks of bacterial diseases.

ACKNOWLEDGMENTS

This work was supported by the National Fishery and Aquaculture Institute (INAPESCA) and contributions from shrimp farmers.

Fitmar Co. provided the shrimp used in the bioassays. We thank M. Linne for his support, K. Rendon, J. Enciso, C. Bolan, and F. Marrujo for technical assistance, and S. Abad for the microphotographs. Special thanks for their assistance in the field work are extended to J. Cabanillas, A. Galvez, O. Romero, and H. Ramirez from the Aquatic Animal Health Sinaloa State Committee.

REFERENCES

1. **Lightner DV.** 1999. The Penaeid Shrimp Viruses TSV, IHHNV, WSSV, and YHV: current status in the Americas, available diagnostic methods, and management strategies. J Appl Aquacult **9:**27–52. http://dx.doi.org/10.1300/J028v09n02_03.
2. **Del Rio-Rodriguez RE, Soto-Rodriguez S, Lara-Flores M, Cu-Escamilla AD, Gomez-Solano MI.** 2006. A necrotizing hepatopancreatitis (NHP) outbreak in a shrimp farm in Campeche, Mexico: a first case report. Aquaculture **255:**606–209. http://dx.doi.org/10.1016/j.aquaculture.2005.12.014.
3. **Nunan L, Pantoja C, Gomez-Jimenez S, Lightner D.** 2013. "*Candidatus* hepatobacter penaei," an intracellular pathogenic enteric bacterium in the hepatopancreas of the marine shrimp *Penaeus vannamei* (Crustacea: Decapoda). Appl Environ Microbiol **79:**1407–1409. http://dx.doi.org/10.1128/AEM.02425-12.
4. **Soto-Rodriguez SA, Gomez Gil B, Roque A., Lozano R.** 2010. Density of vibrios in hemolymph and hepatopancreas of diseased Pacific white shrimp, *Litopenaeus vannamei*, from northwestern Mexico. J World Aquacult Soc **41:**76–83. http://dx.doi.org/10.1111/j.1749-7345.2009.00335.x.
5. **Jiravanichpaisal P, Miyazaki Limsuwan TC.** 1994. Histopathology, biochemistry and pathogenicity of *Vibrio harveyi* infecting black tiger prawn, *Penaeus monodon*. J Aquat Anim Health **6:**27–35. http://dx.doi.org/10.1577/1548-8667(1994)006<0027:HBAPOV>2.3.CO;2.
6. **Soto-Rodriguez SA, Gomez-Gil B, Lozano R.** 2010. "Bright-red" syndrome in Pacific white shrimp *Litopenaeus vannamei* is caused by *Vibrio harveyi*. Dis Aquat Org **92:**11–19. http://dx.doi.org/10.3354/dao02274.
7. **Soto-Rodriguez SA, Armenta M, Gomez-Gil B.** 2006. Effects of enrofloxacin and florfenicol on survival and bacterial population in an experimental infection with luminescent *Vibrio campbellii* in shrimp larvae of *Litopenaeus vannamei*. Aquaculture **255:**48–54. http://dx.doi.org/10.1016/j.aquaculture.2005.11.035.
8. **Lightner DV, Redman RM, Pantoja CR, Noble BL, Tran LH.** 2012. Early mortality syndrome affects shrimp in Asia. Global Aquacult Advocate **Jan/Feb 2012:**40.
9. **Sritunyalucksana K, Gangnonngiw W, Archakunakorn S, Fegan D, Flegal T.** 2005. Bacterial clearance rate and a new differential hemocyte staining method to assess immunostimulant activity in shrimp. Dis Aquat Org **63:**89–94. http://dx.doi.org/10.3354/dao063089.
10. **Nunan L, Lightner D, Pantoja C, Gomez-Jimenez S.** 2014. Detection of acute hepatopancreatic necrosis disease (AHPND) in Mexico. Dis Aquat Org **111:**81–86. http://dx.doi.org/10.3354/dao02776.
11. **Bell TA, Lightner DV.** 1988. A handbook of normal shrimp histology. Special publication no. 1. World Aquaculture Society, Baton Rouge LA.
12. **Bej AK, Patterson DP, Brasher CW, Vickery MC, Jones DD, Kaysner CA.** 1999. Detection of total and hemolysin-producing *Vibrio parahaemolyticus* in shellfish using multiplex PCR amplification of Tl, Tdh and

Trh. J Microbiol Methods **36:**215–225. http://dx.doi.org/10.1016/S0167-7012(99)00037-8.
13. **Joshi J, Srisala J, Truong VH, Chend TI, Nuangsaenge B, Suthienkul O, Lo CF, Flegel TW, Sritunyalucksana K, Thitamadee S.** 2014. Variation in *Vibrio parahaemolyticus* isolates from a single Thai shrimp farm experiencing an outbreak of acute hepatopancreatic necrosis disease (AHPND). Aquaculture 428-429:297–302. http://dx.doi.org/10.1016/j.aquaculture.2014.03.030.
14. **Sirikharin R, Taengchaiyaphum S, Sritunyalucksana K, Thitamadee S, Flegel TW, Mavichak R.** 2014. A new and improved PCR method for detection of AHPND bacteria. http://www.enaca.org/modules/news/article.php?article_id=2030&title=new-pcr-detection-method-for-ahpnd.
15. **Gomez-Gil B, Soto-Rodríguez S, Lozano R, Betancourt-Lozano M.** 2014. Draft genome sequence of *Vibrio parahaemolyticus* strain M0605, which causes severe mortalities of shrimps in Mexico. Genome Announc **2**(2):e00055-14. http://dx.doi.org/10.1128/genomeA.00055-14.
16. **Gomez-Gil B, Soto-Rodriguez S, Garcia-Gasca A, Roque A, Vazquez-Juarez R, Thompson FL, Swings J.** 2004. Molecular identification of *Vibrio harveyi*-related isolates associated with diseased aquatic organisms. Microbiology **150:**1769–1777. http://dx.doi.org/10.1099/mic.0.26797-0.
17. **Kosman E, Leonard KJ.** 2005. Similarity coefficients for molecular markers in studies of genetic relationships between individuals for haploid, diploid, and polyploid species. Mol Ecol **14:**415–424. http://dx.doi.org/10.1111/j.1365-294X.2005.02416.x.
18. **Tran L, Nunan L, Redman RM, Mohney LL, Pantoja CR, Fitzsimmons K, Lightner DV.** 2013. Determination of the infectious nature of the agent of acute hepatopancreatic necrosis syndrome affecting penaeid shrimp. Dis Aquat Org **105:**45–55. http://dx.doi.org/10.3354/dao02621.
19. **Cabanillas-Beltran H, LLausas-Magaña E, Romero R, Espinoza A, Garcia-Gasca A, Nishibuchi M, Ishibashi M, Gomez-Gil B.** 2006. Outbreak of gastroenteritis caused by the pandemic *Vibrio parahaemolyticus* O3: K6 in Mexico. FEMS Microbiol Lett **265:**76–80. http://dx.doi.org/10.1111/j.1574-6968.2006.00475.x.
20. **Ibarra-Gamez JC, Galaviz-Silva L, Molina-Garza ZJ.** 2007. Distribution of necrotizing hepatopancreatitis bacterium (NHPB) in cultured white shrimp, Litopenaeus vannamei, from Mexico. Ciencias Mar **33:**1–9.
21. **Lightner DV.** 1996. A handbook of shrimp pathology and diagnostic procedures for disease of cultured penaeid shrimp. World Aquaculture Society, Baton Rouge, LA.
22. **Frelier FP, Sis RF, Bell TA, Lewis DH.** 1992. Microscopic and ultrastructural studies of necrotizing hepatopancreatitis in Pacific white shrimp (*Penaeus vannamei*) cultured in Texas. Vet Pathol **29:**269–277. http://dx.doi.org/10.1177/030098589202900401.
23. **Vincent AG, Lotz JM.** 2005. Time course of necrotizing hepatopancreatitis (NHP) in experimentally infected *Litopenaeus vannamei* and quantification of NHP bacterium using real-time PCR. Dis Aquat Org **67:**163–169. http://dx.doi.org/10.3354/dao067163.
24. **Vincent AG, Breland VM, Lotz JM.** 2004. Experimental infection of Pacific white shrimp *Litopenaeus vannamei* with necrotizing hepatopancreatitis (NHP) bacterium by *per os* exposure. Dis Aquat Org **61:**227–233. http://dx.doi.org/10.3354/dao061227.
25. **Soto-Rodriguez SA, Gomez-Gil B. Lozano R, del Rio-Rodriguez R, Diéguez AL, Romalde JL.** 2012. Virulence of *Vibrio harveyi* responsible for the "bright-red" syndrome in the Pacific white shrimp *Litopenaeus vannamei*. J Invertebr Pathol **109:**307–317. http://dx.doi.org/10.1016/j.jip.2012.01.006.
26. **Alday-Sanz V, Roque A, Turnbull JF.** 2002. Clearing mechanisms of *Vibrio vulnificus* biotype I in the black tiger shrimp *Penaeus monodon*. Dis Aquat Org **48:**91–99. http://dx.doi.org/10.3354/dao048091.
27. **Hauton C.** 2012. The scope of the crustacean immune system for disease control. J Invertebr Pathol **110:**251–260. http://dx.doi.org/10.1016/j.jip.2012.03.005.
28. **Jiravanichpaisal P, Lee BL, Söderhäll K.** 2006. Cell-mediated immunity in arthropods: hematopoiesis, coagulation and opsonization. Immunobiology **211:**213–236. http://dx.doi.org/10.1016/j.imbio.2005.10.015.
29. **Lin X, Söderhäll I.** 2011. Crustacean hematopoeisis and the astakine cytokines. Blood **117:**6417–6424. http://dx.doi.org/10.1182/blood-2010-11-320614.
30. **Aguirre-Guzman G, Vazquez-Juarez R, Ascencio F.** 2001. Differences in the susceptibility of American white shrimp larval substages (*Litopenaeus vannamei*) to four species. J Invertebr Pathol **78:**215–219. http://dx.doi.org/10.1006/jipa.2001.5073.
31. Reference deleted.
32. **Waterfield N, Kamita SG, Hammock BD, Ffrench-Constant R.** 2005. The *Photorhabdus* Pir toxins are similar to a developmentally regulated insect protein but show no juvenile hormone esterase activity. FEMS Microbiol Lett **245:**47–52. http://dx.doi.org/10.1016/j.femsle.2005.02.018.
33. Reference deleted.
34. **Martin GG, Rubin N, Swanson E.** 2004. *Vibrio parahaemolyticus* and *V. harveyi* cause detachment of the epithelium from the midgut trunk of the penaeid shrimp *Sicyonia ingentis*. Dis Aquat Org **60:**21–29. http://dx.doi.org/10.3354/dao060021.
35. Reference deleted.
36. Reference deleted.
37. **Saulnier D, Haffner P, Goarant C, Levy P, Ansquer D.** 2000. Experimental infection models for shrimp vibriosis studies: a review. Aquaculture **191:**133–144. http://dx.doi.org/10.1016/S0044-8486(00)00423-3.
38. **FAO.** 2013. Report of the FAO/MARD technical workshop on early mortality syndrome (EMS) or acute hepatopancreatic necrosis syndrome (AHPNS) of cultured shrimp (under TCP/VIE/3304), Hanoi, Vietnam, 25 to 27 June 2013. FAO Fisheries and Aquaculture report no. 1053. FAO, Rome, Italy.
39. **Comision Nacional de Acuacultura y Pesca, SAGARPA.** 2005. Anuario estadistico de acuacultura y pesca. Comision Nacional de Acuacultura y Pesca, SAGARPA, Mazatlán, México.
40. **Comision Nacional de Acuacultura y Pesca, SAGARPA.** 2011. Anuario estadistico de acuacultura y pesca. Comision Nacional de Acuacultura y Pesca, SAGARPA, Mazatlán, Mexico.